

# New Miller Codes for Run-Length Control in Visible Light Communications

Xuanxuan Lu and Jing Li (Tiffany)

**Abstract**—Designing run-length limited (RLL) codes for visible light communication systems must account for multiple performance factors including spectral efficiency, power efficiency, DC balance, and flicker avoidance. This paper reports a new class of enhanced Miller codes, termed eMiller codes, which are capable of achieving highly desirable performances in all of these accounts. An improved Viterbi algorithm (VA), termed *mnVA*, is developed to help further enhance the performance of eMiller codes by preserving multiple candidate sequences at each decoding stage. This performance-enhancing algorithm introduces little complexity increase compared to the original VA. Analysis on flicker control, power spectral density and minimum Hamming distance demonstrates the all-around wellness of these new codes. Extensive simulations are carried out to evaluate eMiller codes by themselves and in practical VLC systems. It is shown that the original VA already allows eMiller codes to deliver a performance noticeably better than conventional Miller and FM0/FM1 codes (and on par with Manchester codes). This result is particularly exciting, as eMiller codes are also more spectral efficient than Manchester codes. The *mnVA* further allows eMiller codes to surpass Manchester codes and 4B6B codes in practical RS-coded VLC systems. Simulation results confirm the superb performance of the RS-eMiller schemes.

**Index Terms**—Visible light communications, run-length limited codes, bandwidth efficiency, power efficiency.

## I. INTRODUCTION

Spurred by the recent advances in solid-state lighting, visible light communications (VLC) is becoming an increasingly attractive technology for indoor high-rate data transmission [1] [2]. Utilizing the visible light spectrum from 380 to 780 nm, VLC provides the potential for multi-gigabit data rate connection with little adverse impact on human health [3] [4] [5]. It is also proposed as a viable option for use with Wi-Fi to produce high-speed reliable communications for laptops, cell-phones and tablets in indoor spaces [6]. Since a single LED (light-emitting diodes) system is loaded with dual tasks of illumination and communication, the successful realization of VLC technology is expected to provide good dimming and flicker control and, at the same time, deliver low bit error rate (BER) and high spectral efficiency [7] [8] [10]. Hence, as standardized by IEEE 802.15.7, a VLC system should include two essential components: run-length limited (RLL) codes and forward error correction (FEC) codes [11].

This work was supported by National Science Foundation under Grants No.0928092, 1133027 and 1343372.

The authors are with the Department of Electrical and Computer Engineering, Lehigh University, Bethlehem, PA 18015 USA. (e-mail: xul311@lehigh.edu; jingli@ece.lehigh.edu).

Part of the work of Li was performed while she was visiting Tongji University, China.

Digital Object Identifier: 10.1109/TWC.2018.2785398

A rich variety of FEC codes have been explored for VLC systems to achieve reliable transmission, and, if possible, to perform some level of dimming control<sup>1</sup>. Noteworthy examples include modified Reed Muller (RM) codes based on minimal compensate symbols (CS) [12], conventional Reed-Muller codes based on the bent function [13], rate-compatible convolutional codes [14], low density parity-check (LDPC) codes [15], and turbo codes [16].

In comparison, the RLL study in VLC is rather scant. Run-length constraints bound the length of stretches (runs) of repeated bits during which the signal does not change between consecutive transitions. RLL codes are used to exclude the appearance of certain prescribed sequences from the string of symbols transmitted (e.g. [17] [18] [19]), in order to prevent the precluded sequences from causing detrimental errors, such as severe inter-symbol interference (ISI) and loss of synchronization clocks. In the context of VLC, RLL codes take in random data symbols at the input, and eliminate long runs of 0's and 1's to help recover the synchronization clock, provide good DC balance, and avoid LED flickers.

Previous studies on RLL codes have been largely driven by the digital recording application, with little consideration to VLC application. Most of the practical RLL codes available in the literature, including Manchester codes, 4B6B, 8B10B, and FM0/FM1 codes [11] [20], have not been specifically evaluated nor optimized in the VLC context. The exceptions are three recent studies by Wang and Kim [21] [22], and by Lu and Li [23]. Both studies considered RLL coding deployed in combination with FEC coding in VLC systems. Specifically, the pioneering work of [21] developed a soft-input hard-output (SIHO) decoding strategy for the 4B6B RLL codes that can produce multiple decoding candidates, and shows its good performance in a hard Reed-Solomon (RS) decoded VLC system. Then [22] proposed a soft-input soft output (SISO) decoding strategy for the 4B6B codes, and demonstrated its effectiveness in a soft RS decoded VLC system. The more recent study of [23] exploited the renowned “turbo paradigm” by constructing an interleaved serially-concatenated coding system employing an inner Miller RLL code and an outer convolutional code and developing a soft-iterative (BCJR-based) decoding algorithm. It was shown that, while Miller codes are fairly weak when used alone, combined with outer codes they can together form a powerful cascaded structure capable of interleaving gains that surpass the existing RLL- and FEC-coded VLC systems reported in the literature [21].

<sup>1</sup>Almost all of the studies were purely devoted to FEC without including RLL investigation.

While the work of [21], [22] and [23] have presented interesting findings, all focused on the decoding aspect of RLL codes. The primary contribution of this paper is the invention of a new class of Miller codes, termed *enhanced Miller codes* or *eMiller codes*, which preserve all the pros of conventional Miller codes without the cons. Indeed, the single biggest reason that prevents conventional Miller codes from being widely deployed in practical systems – despite their highly-desirable spectrum efficiency and linear-time soft decodability – is the disappointing bit error rate (BER) that puts them far behind Manchester codes and FM0/FM1 codes [24] [25] [26].

In this paper, our contribution includes: 1) we first construct the new code using state diagram, and propose a new design, which results in a class of *systematic* Miller codes that are both *spectrum efficient and power efficient*. The minimum distance of eMiller codes is computed, which, being far larger than that of the conventional construction, clearly explains their superb performance; 2) We analyze the DC balance and the flicker control of the new proposed code to show the feasibility of eMiller codes for VLC application. We theoretically calculate the power spectrum density (PSD) to verify the spectrum efficiency of the eMiller codes as well; 3) On the decoding aspect, exploiting the trellis structure, we propose a modification to the original Viterbi algorithm (VA) that allows for multiple survival paths. The new algorithm, thereafter referred to as *mn* Viterbi algorithm (*mnVA*), preserves *m* best candidates at each intermediate decoding stage and *n* best survivors at the final decoding stage. We compare the complexity of the proposed *mnVA* with the original VA and the maximum likelihood (ML) decoding algorithm. It is worth noting that this performance-enhancing modification introduces very little additional computational complexity and memory size increase (linear with the *m* and *n*) to the original VA, and the major cost is more time for comparison operation.

The performance of the proposed eMiller codes are evaluated in both channel-coded and uncoded VLC systems. In the uncoded systems, we show that eMiller codes, with classic Viterbi algorithm, can already deliver a BER performance that is noticeably better than conventional Miller codes and FM0/FM1 codes, and on par with Manchester codes. This result is exciting, because Manchester codes, with the so-called 3 dB advantage [26], are the best-performing practical rate-1/2 RLL codes known to date. The eMiller codes (with *mnVA* decoding) therefore boast not only good power efficiency, but also high spectral efficiency!

In the coded systems, we consider the use of Reed-Solomon (RS) codes for forward error correction. The elegant trellis structure of eMiller codes lends themselves to an efficient SISO decoding algorithms, which has linear-time complexity, delivers ML optimality, and offers a variant that can produce soft outputs (i.e., BCJR algorithm). The eMiller codes with BCJR decoding is able to achieve good performance by feeding soft information to the RS decoder. However, RLL codes may be used with different kinds of forward error correction (FEC) codes in practical systems. Some FEC codes can be soft decoded with a low enough complexity, but some can not. For example RS codes used here. The

complexity of the soft decoding of RS codes is much higher compared to the well known Berlekamp-Massey (BM) (hard) decoding algorithm, which prevents the soft RS decoding from being widely employed in industry. We therefore consider the eMiller codes with both BCJR decoding and *mn* VA. For the hard RS decoding cases (BM decoding), the proposed RS-eMiller scheme with *mnVA* outperforms the RS-Manchester scheme, the conventional RS-Miller scheme, as well as an RS-4B6B scheme presented in [21]. Note that the 4B6B codes are decoded using the algorithm proposed in [21], which is a soft ML decoding algorithm with multiple survival paths and which has a complexity increasing exponentially with the block size. When conjunction with the soft RS decoder, our eMiller-RS scheme with BCJR decoding algorithm still clearly performs better than the RS-4B6B scheme in [22] because of the good error correction ability of the eMiller codes. For a fair comparison, we have adjusted the rate of the RS codes to ensure that all the schemes have approximately the same overall code rate and the same block size. That RS-eMiller scheme delivers the best performance among all of these existing schemes, which speaks strongly for the effectiveness of the new codes.

The rest of the paper is organized as follows. Section II introduces the VLC system model. Section III presents the new eMiller codes. Section IV analyzes the new codes and compares them with several frequently-used RLL codes including Manchester codes, FM0/FM1 codes, and classic Miller codes. Section V presents the proposed *mn* Viterbi decoding algorithm. Section VI presents the simulation results for both the uncoded and the coded VLC systems, and Section VII concludes the paper.

## II. SYSTEM MODEL

Consider the VLC system shown in Fig. 1, which consists of a run-length limited code, an on-off keying (OOK) modulation and an optional forward error correction code. It is noted here we propose to use the OOK modulation, because of the simplicity of the modulation scheme as stated in the IEEE 802.15.7 VLC standard. The brightness control can be realized in the module of OOK modulation by controlling the brightness of OOK waveform, or add compensation symbols. Other advanced brightness control methods like pulse position modulation are possible to be considered for future work.

The channel-coded system is shown in the red dot-dashed box and the uncoded system is shown in the blue dashed box. As stated in the IEEE standard, RS codes are preferred over the more advanced coding schemes such as LDPC codes [27] and turbo codes in order to support short data frames, achieve low coding complexity and interface well with RLL codes. Hence, in this paper we consider RS codes as the forward error correction mechanism for VLC. The VLC channel is modeled as an additive white Gaussian noise (AWGN) channel with Gaussian noise  $\mathbf{n} \sim \mathcal{N}(\mathbf{0}, \sigma^2)$ . Let  $\mathbf{x}$  be the (possibly FEC-coded,) RLL-coded and OOK-modulated signals the sender puts on the VLC channel, and let  $\mathbf{y} = \mathbf{x} + \mathbf{n}$  be the signal at the receiver photodiode (PD). Our goal in this paper is to explore good RLL codes (as well as appropriate decoding

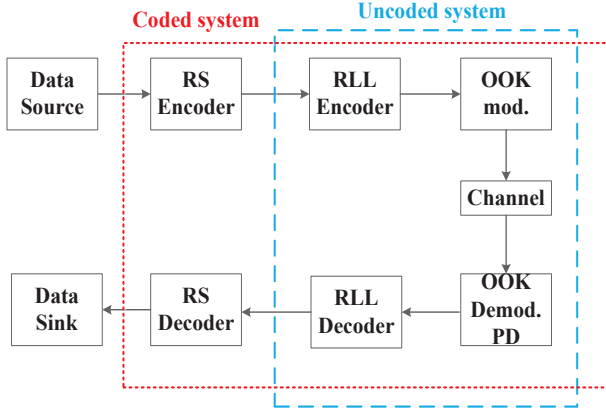


Fig. 1: VLC system model

algorithms) to help the VLC receiver achieve high power efficiency and high spectrum efficiency.

### III. NEW CLASS OF ENHANCED MILLER CODES

#### A. Conventional Miller Codes

Miller codes, also known as delay modulation, are a class of RLL codes that guarantee at least one transition every two bit interval and never more than two transitions every two bit interval. They have memory, and hence lend themselves to convenient trellis representation and maximum-likelihood (ML) decoding via the Viterbi algorithm. The biggest advantage of Miller codes is their high spectrum efficiency, as they require only about half the bandwidth (considering main-lobe bandwidth) of Manchester RLL codes and FM0/FM1 RLL codes [24] [26]. This can be highly desirable especially for VLC systems aiming to support giga-bit data rate, as the light-emitting diodes (LED) used in VLC are typically bandwidth limited to a couple of hundred MHz. Despite of this spectral advantage, however, Millers are seldom explored in practical systems, due to their rather poor power efficiency that sets their BER performance far behind that of Manchester and FM0/FM1 codes [26].

Figure 2 demonstrates the trellis structure of Miller codes<sup>2</sup>. Miller codes may be viewed as rate-1/2 convolutional codes where one information binary digit is encoded into two coded binary digits based on the state diagram. Using the method developed for convolutional codes, we can compute the “free distance” of Miller codes, which turns out to be only 1. This explains their rather disappointing BER performance. Their error rate performance (at high signal-to-noise ratio (SNR)) under AWGN channel can therefore be approximated by

$$P_{Miller}(E) \approx Q\left(\sqrt{\frac{E_b}{N_0}}\right), \quad (1)$$

where  $Q(x)$  is the Gaussian probability integral,  $E_b/N_0$  is the signal energy-to-noise spectral density ratio, and  $N_0/2 = \sigma^2$  is the variance of the additive Gaussian noise.

<sup>2</sup>Please note that the Fig. 1 of Ref. [23] is corrected to the Fig. 2 in this paper.

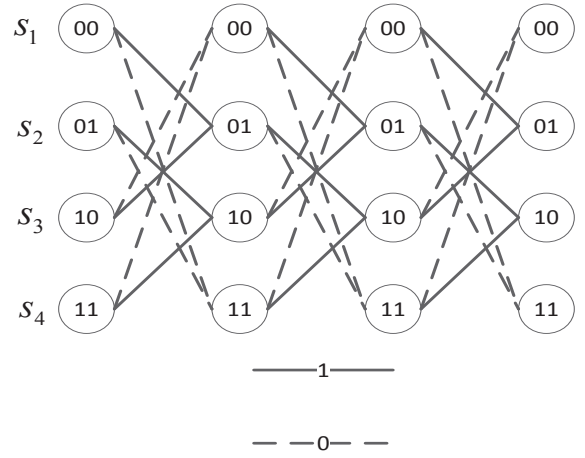


Fig. 2: Trellis diagram of conventional Miller codes. At each stage, the dash line is associated with input 0, and the solid line is associated with input 1. The encoded output takes the same value as the next state.

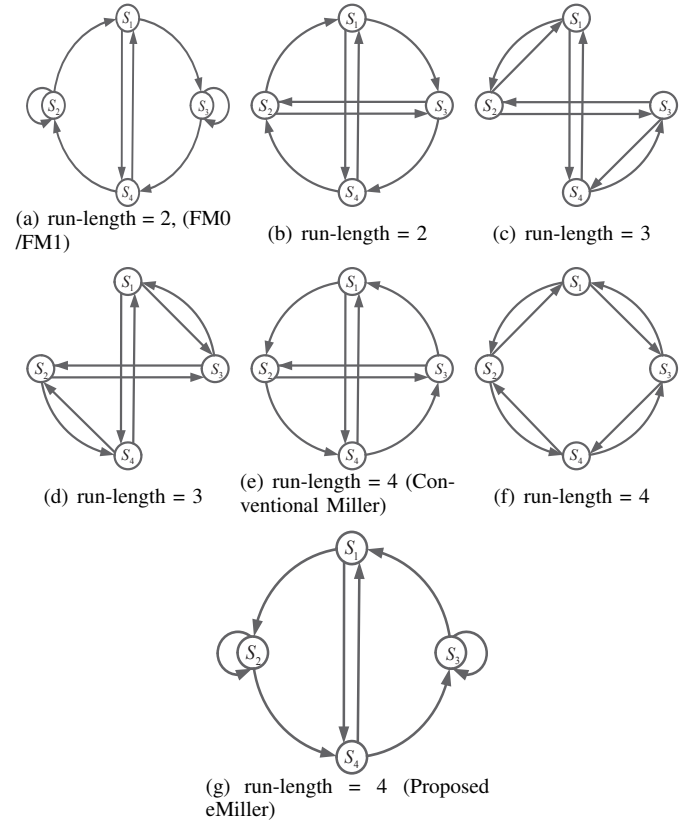


Fig. 3: State diagram of trellis-based RLL codes with run-length 2, 3, 4.

#### B. Proposed New Class of Enhanced Miller Codes

Having analyzed the pros and cons of conventional Miller codes, we now work to improve their power efficiency while preserving their spectrum efficiency. Recall that a 4-state convolutional code (which appears to have a similar trellis structure as Miller codes) can have a free distance as large as 5 (e.g.  $(1+D+D^2, 1+D^2)$ ), there is good reason to believe that by adjusting the trellis structure, it is possible to increase the

minimum distance of Miller codes while maintaining the same (or similar) run-length constraint. Unlike convolutional codes that are linear, RLL codes cannot be linear codes (for example, the all-zero sequence is never a valid output). The free distance (or the minimum distance) and the run-length constraint are two competing factors that must be well balanced in an RLL code.

A class of practical RLL code candidates with one input and two outputs is investigated. For simplicity, we assume the output takes the same value as the next state as other peer RLL codes like the FM0/FM1 code, Miller code and so on. Although possible computer-aided exhaustive search can be used to find a good candidate code with good distance performance, it is cumbersome to use brute-force computer search to find the best candidate accommodating multiple performance factors including minimum distance, flickering, DC balance and run-length limit. We show that the process can be significantly simplified by judicious analysis. We leverage the state diagram to derive the trellis-based RLL codes with the best bit error rate performance. Let  $S_1$ ,  $S_2$ ,  $S_3$  and  $S_4$  denote the state 00, 01, 10 and 11.

We first consider possible codewords with run-length 2. Clearly the outputs from state  $S_1$  (00) could only be  $S_3$  (10) and  $S_4$  (11) (if the next state goes to  $S_2$  (01) or  $S_1$  (00), the run-length would be greater than 2). Following the same line of reasoning, we can construct the state transition for state  $S_2$ ,  $S_3$  and  $S_4$ . The only possible state diagram of the trellis-based RLL codes is shown in Fig. 3 (a). It is essentially the FM0/1 code, which would be detailed in the next section. Similarly, we provide the possible RLL codewords with run-length 3 in Fig. 3 (b)(c). However, it is clear that the minimum distance of these codes is still 1 as the conventional Miller code, which is undesirable.

*Lemma 1: The maximum run-length for the RLL trellis code with one input and two outputs is 4. When run-length is 4, the state diagram consists of path  $S_1 \rightarrow S_2 \rightarrow S_4 \rightarrow S_3 \rightarrow S_1$ .*

*Proof:* First of all, the RLL constraint eliminates such connections as  $00 \rightarrow 00$  and  $11 \rightarrow 11$ . The paths that produce the largest run-length are therefore  $01 \rightarrow 11 \rightarrow 10$  and  $10 \rightarrow 00 \rightarrow 01$ , with yield a maximum run-length of 4. ■

Lemma 1 states that a rate 1/2 trellis code can only have a maximum run-length of 2, 3, or 4. Using the basic reasoning for RLL and the symmetry rule, we plot in Fig. 3 all the possible state diagrams in accordance to an RLL of 2, 3, and 4, respectively. It is easy to verify that  $d_{min}$  for these seven state diagrams is 2, 1, 1, 1, 1, 1, and 2, respectively. Among the two state diagrams that produce the larger  $d_{min}$ , we see that the one depicted in Fig. 3(a) actually corresponds to the FM0/FM1 code, and that the one depicted in Fig. 3(f) demonstrates a new class of codes which we call *enhanced Miller codes*.

The trellis structure of eMiller codes is shown in Fig. 3 (f). We see that these eMiller codes enjoy the same structure property as the conventional Miller codes (i.e. at least one transition, but never more than two, every two bit intervals), and produce the same PSD, but promise a better free distance of 2-which doubles that of the conventional Miller codes and on par with that of Manchester codes and FM0/FM1 codes. The error rate of eMiller codes under AWGN channel at high

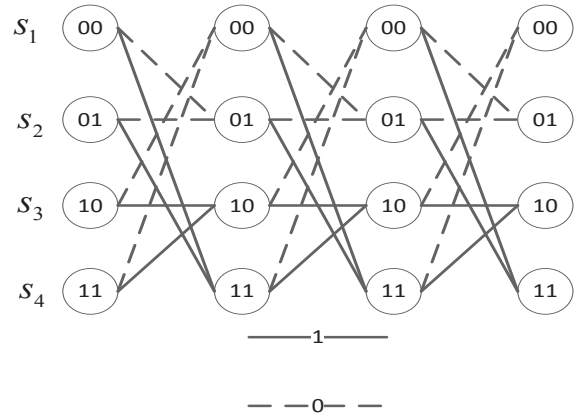


Fig. 4: Trellis diagram of eMiller codes. Dash lines are associated with input 0, and solid lines are associated with input 1. The encoded output takes the same as the next state.

SNR can therefore be approximated by

$$P_{eMiller}(E) \approx Q\left(\sqrt{\frac{2E_b}{N_0}}\right). \quad (2)$$

#### IV. ANALYSIS AND COMPARISON

In this section, we will analyze the new eMiller codes and compare them with conventional Miller codes as well as other commensurable peers. We will proceed to decoding issues and evaluate the true performance of these codes in the next section.

We start by briefing two important classes of rate-1/2 RLL codes that will provide meaningful comparison and/or contrast to our new codes.

##### • Manchester Codes

Manchester codes are a popular class of RLL codes that have also gotten into the IEEE 802.15.7 standard. Also known as biphasic codes or split-phase codes, Manchester codes are simple and memoryless RLL codes, whose output symbols always have a transition in the middle. For example, in Manchester coding, an information bit “1” may be represented by a half-symbol-wide “on” pulse followed by a half-symbol-wide “off” pulse, and an information bit “0” represented the other way around. Clearly Manchester codes provide an excellent clock recovery signal, a run-length limit of 1 bit interval (2 half-bits), and a precise DC balance of 50%. When viewed as a rate-1/2 code, Manchester codes clearly possess a minimum distance of 2. The probability of error is identical to that of a non-return-to-zero (NRZ) coded system or an OOK system, which can be precisely evaluated as:

$$P_{Manchester}(E) = Q\left(\sqrt{\frac{2E_b}{N_0}}\right). \quad (3)$$

Manchester codes can also be described by a 2-state trellis, as shown in Fig. 5. The Manchester codes have no memory. Hence, decoding can use a straight-forward symbol-by-symbol ML detection process (which is basically minimum distance comparison on AWGN channels), or trellis-based Viterbi algorithm.

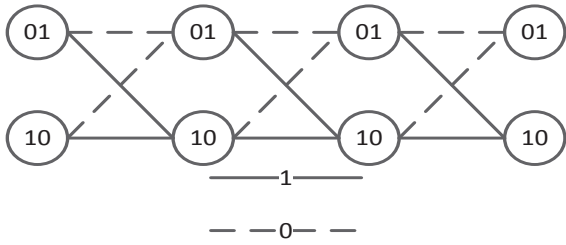


Fig. 5: Trellis diagram of Manchester codes. Dash lines are associated with input 0, and solid lines are associated with input 1. The encoded output takes the same as the next state.

#### • FM0/FM1 Line Codes

Two other classes of relevant RLL codes are FM0 and FM1 codes, which are typically used in lieu of Manchester codes when dealing with noncoherent communication [26]. FM1 line codes, also termed *biphase mark*, require a transition be always present at the beginning of each bit. An information bit “1” is encoded as a second transition in the middle of the bit interval and an information bit “0” is encoded as no second transition in the bit interval. This results in representing the bit “1” by one of the two Manchester symbols, and representing the bit “0” by one of the two NRZ symbols. FM0 codes, also known as *biphase space*, are essentially FM1 codes with the representation of “1” and “0” interchanged.

Clearly, FM0/FM1 codes are codes with memory. As shown by their trellis structure in Fig. 6, the free distance is 2, and the asymptotic error probability at high SNR may be approximated as

$$P_{FM0/FM1}(E) \approx Q\left(\sqrt{\frac{2E_b}{N_0}}\right). \quad (4)$$

Note that this is a lower bound. The actual performance of FM0/FM1 (using ML Viterbi algorithm) is worse than that of Manchester codes (as will be shown later). This is because, from a particular perspective, FM0/FM1 codes may be treated as a half-bit time shift version of Manchester codes, or, a differentially-encoded version of Manchester codes [26].

It also follows that FM0/FM1 codes have the same run-length control (i.e., 2 half-bits) and the same power spectrum as Manchester codes, since a time shift in the observation has no effect on run-length nor power spectrum.

#### A. DC Balance and Flicker Analysis

The VLC technology achieves cost-effectiveness by overloading the communication function to an LED illumination system. However, communication, being secondary, must not induce severe negative impact on the primary role of illumination. To ensure a proper lighting function, flickering mitigation and dimming control should be considered in a VLC system.

Regarding DC balance, the desired goal is to achieve a consistent 50% brightness during the course of data transmission. Manchester codes are particularly good in this, as they always provide a 50% DC balance regardless of the sequence size. In comparison, the proposed eMiller codes, the conventional Miller codes, and the FM0/FM1 codes have exactly the same

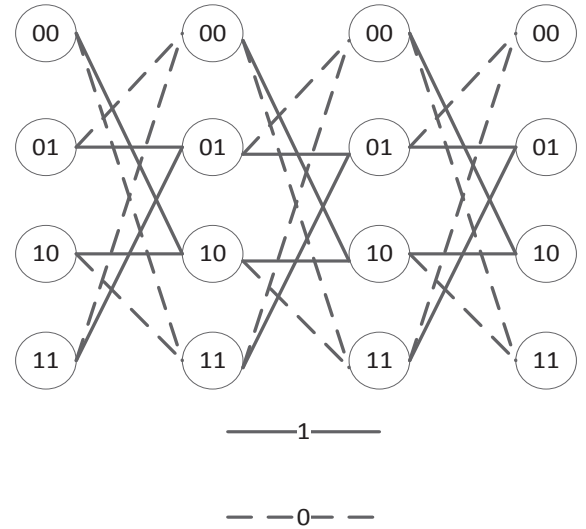


Fig. 6: Trellis diagram of FM1 codes. Dash lines are associated with input 0, and solid lines are associated with input 1. The encoded output takes the same as the next state.

brightness characteristics and, compared to Manchester codes, their DC-balancing capability is slightly worse (especially for very short sequences). For convenience, we introduce the concept of “super-symbol( $M$ )”, which is formed by  $M$  consecutive bits. As long as the super-symbol interval is shorter than the maximum flicking time period (MFTP) which is about 5ms [1], it is sufficient to evaluate the DC-balance (as well as the flickering issue) at the super-symbol level rather than the individual bit level. Fig. 7, 8 and 9 show the super-symbol brightness in the conventional Miller codes, the FM0/FM1 codes and eMiller codes, respectively. The size of the super-symbol increases from  $M = 10$  to 100, 300 and 500 bits. For the low-rate applications, in which small super-symbol sizes is considered to satisfy MFTP, such as billboard communication, the disadvantage of FM0/FM1 and conventional Miller codes is very obvious. FM0/FM1 and conventional Miller codes may not be able to provide the DC balancing performance meeting requirements. For the advanced high-speed systems, like VLC systems with data rate 100 Mbit/s, all the super-symbols considered satisfy the MFTP. As illustrated by the histograms in all the three figures, the brightness intensity of the super-symbols becomes increasingly uniform and approaches the desirable level of 50% when  $M$  increases. The DC balance performance of Miller and FM0/FM1 can catch up. However, the brightness of the super-symbols coded by our proposed eMiller codes converges to 50% quickly than the conventional Miller codes, and FM0/FM1 codes. It can be observed that there is still fluctuation in brightness using the conventional Miller codes, and FM0/FM1 codes when  $M = 300$ . The brightness level of our proposed eMiller codes becomes fairly consistent (50%). Though the difference of the performance among these schemes is not significant, but the DC balance of the our proposed eMiller codes is still slightly better than the Miller and FM0/FM1 codes.

A related issue is flicker, caused by the light intensity (or brightness) change between every two super-symbols. It

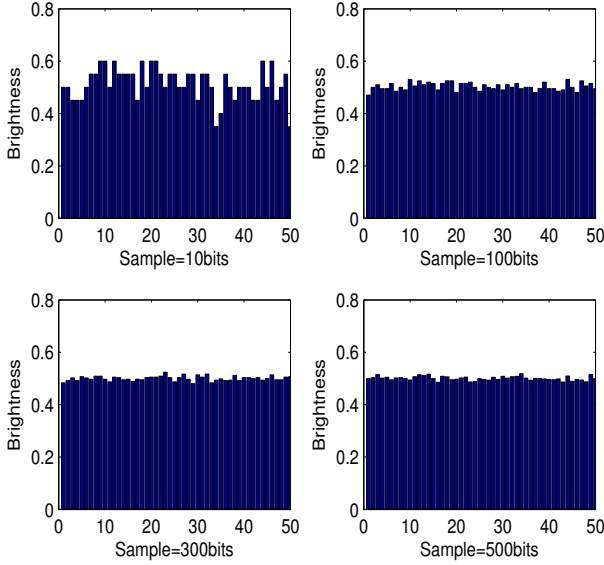


Fig. 7: Brightness in conventional Miller codes with different super-symbol size  $M = 10, 100, 300, 500$ .

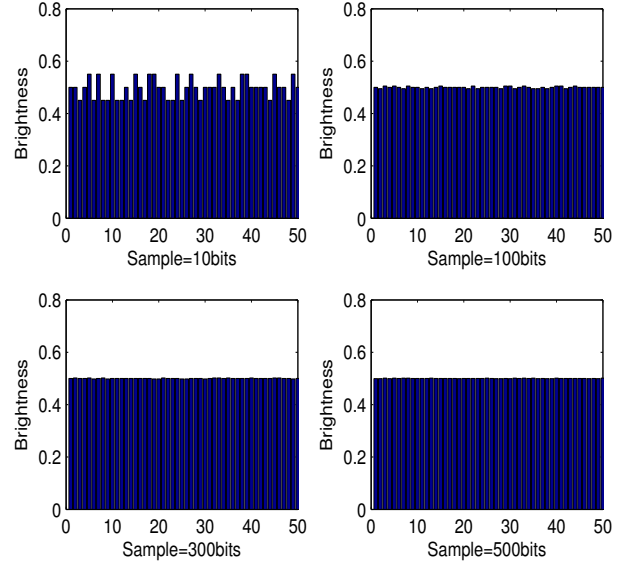


Fig. 8: Brightness in FM0/FM1 codes with different super-symbol size  $M = 10, 100, 300, 500$ .

is generally recognized that light intensity change with a frequency higher than  $1/MFTP$  is beyond human eye perception and the flicker issue thereof can be safely ignored [1]. Considering that super-symbol( $M$ )'s delivers a fairly uniform brightness level in eMiller codes, as shown in Fig. 9, the flicker mitigation can be properly handled.

Brightness control is a good feature of visible light communication. In VLC, communication function is added over the illumination function of the LED lights. For purely brightness control, there are many ways to realize it. As stated in the standard IEEE 802.15.7, several widely accepted ways are adding compensation symbols, controlling the brightness for on-off keying (OOK), using different kinds of pulse position modulation (PPM) and so on. Each method has both its own pros and cons. However, all the brightness-control methods have no error correction ability. Our proposed eMiller code is designed to provide strong error-control ability and good bandwidth efficiency to achieve reliable and efficient transmission, which is fundamental in communication. It also provides good DC balance and mitigates flicker, which is the basic function of conventional RLL codes in VLC. The eMiller code itself is not for brightness control. However, it is feasible to provide brightness control in our proposed system by adopting all the previously mentioned brightness control methods, such as adding compensation symbols, PPM and so on, with the eMiller code (For simplicity, we consider OOK modulation in our paper, as reference [21][22][25]). All the dimming control methods applied to other RLL codes (like Miller codes, Manchester codes and so on) can be applied to our eMiller codes. Designing other innovative dimming control methods is also an interesting topic for future work.

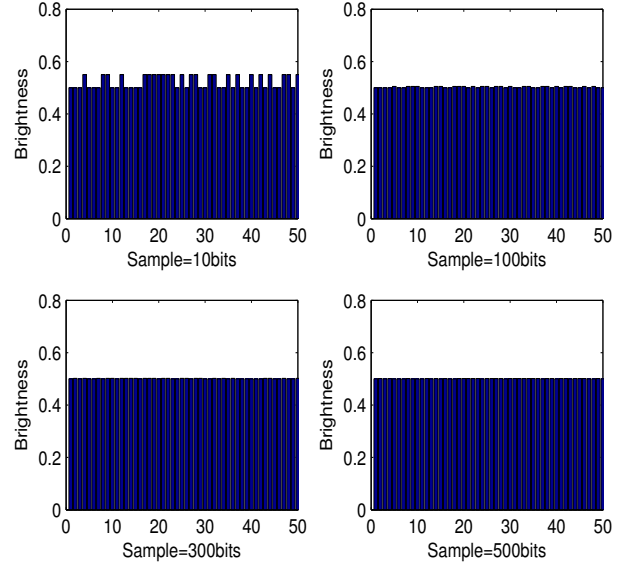


Fig. 9: Brightness in eMiller codes with different super-symbol size  $M = 10, 100, 300, 500$ .

### B. Power Spectrum Density Analysis

Spectral efficiency is an important parameter that measures the quality of signal transmission systems, which refers to the use of a radio frequency spectrum in more efficient ways. Since frequency bands become increasingly crowded, how to use radio frequency bands more efficiently has to be considered in all kinds of modern communication systems, including visible light communication systems. Specially, IEEE 802.15.7 standards specifies the coexistence five adjacent channels [1] for VLC. The five carriers would overlap under low spectral efficiency cases, making the separation quite difficult and intro-

ducing decoding errors. The second reason for putting priority on the spectrum efficiency in VLC is the usage of multi-color LEDs in VLC. White LEDs can be generated using blue LEDs with yellow phosphor. However, yellow phosphor slows down the switching response of the white LEDs. Alternately, faster white LEDs that can be more useful for communication can be generated by simultaneously exciting red, green and blue LEDs [1]. To better distinguish the different light spectrum at destination, a high spectral efficiency scheme is preferred. As we know, most of the luminaries typically contain multiple LEDs to provide sufficient illumination [1]. These multiple LEDs can be treated as multiple transmitters that can enable visible light MIMO communication to achieve high data rate for the next generation communication. RLL codes with better spectral efficiency is more suitable to be employed in MIMO systems.

To verify the bandwidth efficiency of the proposed eMiller codes, we calculate their power spectral density [9]. The coding rule of the eMiller codes can be described as a first-order Markov random process with four states:  $\mathcal{S}_1=01$ ,  $\mathcal{S}_2=10$ ,  $\mathcal{S}_3=00$ , and  $\mathcal{S}_4=11$ . The system is equally likely to enter into any one of these four states, i.e.,  $p_i = 1/4$ , for  $i = 1, 2, 3, 4$ . The Markov process is then completely described by  $\mathbf{P} = [p_{ij}]$ , the probability-of-transition matrix, where  $p_{i,j}$  denotes the probably of going from state  $\mathcal{S}_i$  to  $\mathcal{S}_j$ . From the coding rule, we can compute the transition matrix as follows

$$\mathbf{P} = \begin{bmatrix} 0.5 & 0 & 0 & 0.5 \\ 0 & 0.5 & 0.5 & 0 \\ 0.5 & 0 & 0 & 0.5 \\ 0 & 0.5 & 0.5 & 0 \end{bmatrix}. \quad (5)$$

Let  $T$  be the symbol interval. The autocorrelation function  $R(\tau)$  (for time separation  $\tau = nT$ , where  $n = 0, 1, 2, \dots$ ) is given by

$$R(nT) = \frac{1}{4} \text{trace}[\mathbf{P}^n \mathbf{W}^T]. \quad (6)$$

where  $\mathbf{W}$  is a square matrix with elements  $w_{i,j} = \int_0^T g_i(t)g_j(t)dt/T$ , and  $g_i(t)$  is the (rectangular) waveform produced when entering state  $\mathcal{S}_i$ . Based on these waveform,  $\mathbf{W}$  can be expressed as

$$\mathbf{W} = \begin{bmatrix} 1 & -1 & 0 & 0 \\ -1 & 1 & 0 & 0 \\ 0 & 0 & 1 & -1 \\ 0 & 0 & -1 & 1 \end{bmatrix}. \quad (7)$$

Substituting  $\mathbf{W}$  and  $\mathbf{P}$  into (6), we get the autocorrelation function of the eMiller-coded sequence

$$R(nT) = \begin{cases} 1, & n = 0 \\ 0, & n \neq 0 \end{cases} \quad (8)$$

Similarly, we can find the autocorrelation for  $\tau = (n + 1/2)T$  as follows:

$$R((n + 1/2)T) = \frac{1}{4} \text{trace}[\mathbf{P}^n \mathbf{W}_1^T] + \frac{1}{4} \text{trace}[\mathbf{P}^{n+1} \mathbf{W}_2^T], \quad (9)$$

where  $\mathbf{W}_1$  is a square matrix with elements  $w_{i,j} = \int_0^{T/2} g_i(t)g_j(t + T/2)dt/T$ , and  $\mathbf{W}_2$  is a square matrix with

elements  $w_{i,j} = \int_{T/2}^T g_i(t)g_j(t + T/2)dt/T$ . We have

$$\mathbf{W}_1 = \begin{bmatrix} -0.5 & 0.5 & 0.5 & -0.5 \\ 0.5 & -0.5 & -0.5 & 0.5 \\ -0.5 & 0.5 & 0.5 & -0.5 \\ 0.5 & -0.5 & -0.5 & 0.5 \end{bmatrix} \quad (10)$$

and

$$\mathbf{W}_2 = \begin{bmatrix} -0.5 & 0.5 & -0.5 & 0.5 \\ 0.5 & -0.5 & 0.5 & -0.5 \\ 0.5 & -0.5 & 0.5 & -0.5 \\ -0.5 & 0.5 & -0.5 & 0.5 \end{bmatrix}. \quad (11)$$

Gathering these relevant equations, we can get the result for autocorrelation function

$$R((n + 1/2)T) = \begin{cases} -0.5, & n = 1 \\ 0, & n \neq 1 \end{cases} \quad (12)$$

By taking the Fourier transform of  $R(\tau)$ , we get the PSD of our eMiller codes:

$$\text{eMiller: } S(f) = A^2 T \left( \frac{\sin(\pi f T / 2)}{\pi f T / 2} \right)^2 \sin^2(3\pi f T / 2), \quad (13)$$

where  $A$  is the signal amplitude (amplitude for the rectangular pulse),  $T$  is the information bit interval, and  $f$  is the frequency for which the PSD is calculated.

In comparison, the PSD of the conventional Miller codes and of Manchester/FM0/FM1 codes<sup>3</sup> can be computed as [24]:

$$\text{Miller: } S(f) = \frac{A^2 T}{2(\pi f T)^2 (17 + 8\cos(2\pi f T))} * (23 - 2\cos(\pi f T) - 22\cos(2\pi f T) - 12\cos(3\pi f T) + 5\cos(4\pi f T) + 12\cos(5\pi f T) + 2\cos(6\pi f T) - 8\cos(7\pi f T) + 2\cos(8\pi f T)); \quad (14)$$

$$\text{Man/FM0/FM1: } S(f) = A^2 T \left( \frac{\sin(\pi f T / 2)}{\pi f T / 2} \right)^2 \sin^2(\pi f T / 2). \quad (15)$$

The PSD curves of these RLL codes are plotted in Fig. 10, where  $T$  and  $A$  are assumed to be unity. All the codes have a fairly small spectral density near frequency zero. Manchester codes and FM0/FM1 codes have identical spectral density, which is not very closely packed around the zero frequency (the DC). With a main lobe less than half the width of that of the Manchester/FM0/FM1 codes, the proposed eMiller codes have its power more concentrated and at a lower frequency, and hence clearly demonstrate a spectrum advantage over these codes. Even with a side lobe, the width of the eMiller codes' lobes is smaller than the Manchester and FM0/FM1 codes' main lobe. As a result, the bandwidth required by eMiller codes is smaller. Compared to the conventional Miller codes, the proposed eMiller codes have a main lobe of a similar width but a bigger side lobe, and hence are slightly less bandwidth efficient than the conventional construction.

Table I provides a quick summary of the various properties

<sup>3</sup>Manchester codes, FM0 codes and FM1 codes have identical PSD.

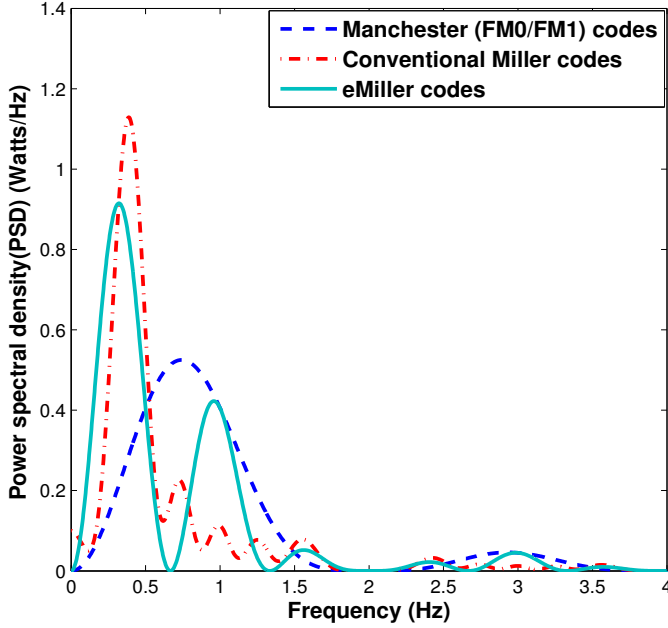


Fig. 10: Power spectral density of Manchester/FM0/FM1, conventional Miller and eMiller codes

for eMiller codes and their rate-1/2 peers<sup>4</sup>. Our eMiller codes clearly stand out as being both energy efficient and spectral efficient. It is noted here the traditional Manchester code and the eMiller code have the same minimum distance and show almost the same performance without forward error codes (FEC) involved in the VLC system. However, the traditional Manchester code has no memory, and the decoding uses the symbol-by-symbol detection. In contrast, the eMiller code has memory size 2 which improves the decoding performance of the serial concatenated FEC-RLL code when concatenated with the FEC. Hence, we rate three  $\sqrt{\quad}$  for the power efficiency of the eMiller codes.

## V. DECODER WITH MULTIPLE SURVIVAL PATHS AND OUTPUTS

### A. Proposed $mn$ Viterbi Decoding Algorithm

We now proceed to the decoding aspect. The trellis structure of eMiller codes lends themselves to an efficient SISO decoding algorithms, which has linear-time complexity, provides ML optimality, and offers a variant that can produce soft outputs (i.e., BCJR algorithm). The eMiller codes with BCJR decoding is able to deliver good performance by feeding soft information to the concatenated FEC decoder. Here we developed an improved SIHO Viterbi decoding algorithm. The motivation is RLL codes may be used with different kinds of forward error

<sup>4</sup>The 4B6B code is not listed in the table, because 4B6B code has a code rate 2/3 instead of 1/2. Every six bits of 4B6B codes have a brightness level 50%. The 4B6B code by itself does not have good error control ability. The concatenation with other error correction codes, like RS codes, may help the decoding. To make a fair comparison, we compare the performance of the (15,5)RS-4B6B (overall code rate 0.22) and the (15,7)RS-eMiller (overall code rate 0.23) codes in Sec. VI.

correction (FEC) codes in practical systems. Some FEC codes can be soft decoded with a low enough complexity, but some can not. For example RS codes. The complexity of the soft decoding of RS codes is much higher compared to the well known Berlekamp-Massey (BM) decoding algorithm, which prevents the soft RS decoding from being widely employed in industry for decades of years.

Viterbi algorithm finds the ML codeword or the path with the best metric. The metric is in general the likelihood of the path, and in the case of AWGN channels, it reduces to (squared) Euclidean distance (soft detection) or Hamming distance (hard detection). Under the assumption that the channel is memoryless, the algorithm traverses through the trellis, and computes the cumulated metric along each path. When two or more paths merge at a state, the path with the best metric so far (survivor path) is retained and the other paths are all eliminated from further consideration. In the final stage, the algorithm selects the single best path among those made into the final state(s).

The improved Viterbi algorithm we discuss here, termed  $mn$ VA, introduces a simple but rather effective modification to the original VA by allowing the decoding states to keep track of multiple survival paths entering them. Let  $L$  be the number of states at each decoding stage ( $L = 4$  for eMiller codes). The conventional VA is essentially an  $(L, 1)$ VA where every intermediate stage retains a total of  $L$  survivors so far (one for each state) and the final stage takes the single best path of all. The new  $mn$ VA allows for the pretension of a total of  $m (\geq L)$  survivors for the intermediate stages and  $n (\geq 1)$  survivors for the last stage ( $n \leq m$ ). It should be noted that while  $mn$ VA generates  $n$  best candidate codewords, it adds very little computational complexity and storage for storing the  $(m - L)$  additional paths to the original VA that produces only 1 decoder output. The major cost is the time of comparison operation which is of linear complexity.

Specific path preserving rule (in the intermediate stages as well as in the final stage) for the proposed  $mn$ VA is given below:

- In the *initialization* phase of the trellis (i.e., the first  $\log_2 L$  time instants), since each state has at the most one branch entering it, no path elimination is performed. The process here is identical to that of the original VA.
- In the *stable* phase where each state is connected to more than one incoming branches/paths, the  $mn$ VA will first compute all the branch metrics pertaining to this time instant  $t$ , and then update all the path metrics (i.e., for time instant  $t$ ) by adding the appropriate branch metrics to the survival paths for the previous time instant ( $t-1$ ). This step is similar to that of the original VA, except that the previous time instant may have up to  $m$  survivors (instead of  $L$  survivors in the original VA). Next, among all the new path metrics, we will select a best path for each one of the current state (which leads to  $L$  survivors), and then take the best  $(m - L)$  paths among the remainders (to make a total of  $m$  survivors).
- In the *final* decision stage, the  $mn$ VA will first update all the path metrics as before, and then declare the  $n$  best ones among these finalists.



TABLE I: Simulated forward schemes

Code	Code rate	Bandwidth efficiency	Power efficiency	DC balancing	Run-length	Clock recovery
Manchester	1/2	✓	✓✓	✓✓✓	2	✓✓✓
FM0/1	1/2	✓	✓	✓	2	✓✓✓
Conventional Miller	1/2	✓✓✓	✓	✓	4	✓✓✓
eMiller	1/2	✓✓	✓✓✓	✓✓	4	✓✓✓

✓ The code with more check means the corresponding performance is better than the peers.

A short summary of the  $mn$ VA goes in the algorithm I.

---

**Algorithm 1**  $mn$  Viterbi algorithm

---

**Input:** Reception from the channel.

**Output:**  $n$  best binary decisions of the length- $N$  original source data.

**Initialization:**

A 4-state trellis corresponding to eMiller code is set up, as shown in Fig. 4.

Each branch is marked with a binary input bit, and two output signals.

All the state metrics are reset to zero.

**Trellis Decoding:**

**for** stage  $t$  from **1** to  $N$  **do**

**for** state  $i$  from **0** to **3** **do**

**for** each branch entering state  $i$  **do**

      compute branch metric as original VA

      add the branch metric to the state metric

**end**

    choose the branch with the smaller metric.

**end**

  choose  $m - 4$  branches with the smallest metric among the branches with the

  larger metric for each state, and keep it.

**end**

Stage  $N$ , trace back the  $n$  survival path; the binary input bits corresponding to the  $n$  survival paths are declared as the input for the RS decoder.

---

As shown in the simulation results (in the next section), by adding one or two more paths at each decoding stage and the final stage, it is enough to bring significant BER performance gain in practical VLC systems. Performance can be further improved by increasing  $m$  and  $n$ , but the complexity increases and the gain is diminishing. Table II quantitatively compares the complexity of the proposed decoder ( $m = 4, 5$  and  $n = 2, m = 6$  and  $n = 4$ ) with both the classic VA ( $m = 4$  and  $n = 1$ ) and the ML decoder. In the table,  $k$  is the corresponding memory size of the codes, and  $N$  is the data block length, which is much larger than  $k$ . The complexity analysis shows that the proposed decoding algorithm does not introduce much complexity and memory size increase compared to the classic VA. The major cost is more time for comparison operation. However, the traditional ML decoder becomes computationally infeasible as the data length increases. It's noted here the computationally-and-resource intensive ML decoder produces

the maximum likelihood codeword among all the possible ( $2^N$ , where  $N$  is the information data length) codewords by calculating the likelihood of all the  $2^N$  codewords. The decoding complexity increases exponentially with the data length  $N$ . The  $mn$ VA decoder leverages the trellis structure of the eMiller codes, keeps  $m$  paths during the decoding stages and produces the most possible  $n$  candidates at the final stage. The complexity per bit increases linearly with the  $m$  and  $n$ . In theory, the  $mn$ VA decoder can retain all the  $m$  paths at each stage. But it is also wasteful and unnecessary to do this in our practical systems. We seek for a good tradeoff between the performance and the complexity.

### B. Code selection in RS decoder

In the channel-coded case (see the VLC system diagram in Fig. 1), the VLC system under consideration is also equipped with an RS code that will be decoded via the well-established BM algorithm.

If the inner RLL code is trellis-based and uses the proposed  $mn$ VA to decode, then  $n$  candidate sequences will be produced and passed to the RS decoder. The RS decoder will run these candidates through, starting from the best candidate to the worst. It will stop as soon as a successful RS decoding is made, as indicated by the CRC (cyclic redundancy check) code that is almost always wrapped around the information data. In the case none of the  $n$  candidates submitted by the  $mn$ VA made a successful pass through the RS decoder (and the CRC check), then the RS decoder output corresponding to the first (the best) candidate will be declared as the final decision.

## VI. SIMULATION RESULTS

We now present computer simulation results to verify the effectiveness of the proposed eMiller RLL codes using the VLC system model depicted in Fig. 1, and compare them with their rate-1/2 peers. Both AWGN and actual VLC channel are considered to verify the efficiency of our proposed codes. For the practical VLC channel, we use the channel environment in [2]. In this scenario, the received signal  $y(t)$  is given by  $y(t) = Rx(t) \otimes h(t) + n(t)$ , where  $x(t)$  represents optical power from LED lighting,  $R$  is the PD conversion efficiency,  $n(t)$  is AWGN,  $h(t)$  is the channel power delay profile (PDP) and  $\otimes$  denotes convolutional operation. A matched filter is added in the OOK demodulator. The room size is  $5\text{m} \times 5\text{m} \times 3\text{m}$ , semi-angle at half power is 70 degree, FOV at a receiver

TABLE II: Complexity comparison of different decoding schemes

# of operations per bit	Add	Compare	Multiplication	Trace back	Memory
Original VA, $m = 4, n = 1$	$2 * 2^k$	$2^k$	$2 * 2^k$	1	$2 * 2^k + \frac{1}{N}$
ML decoder	$\frac{2^N}{N}$	$\frac{2^N - 1}{N}$	$\frac{2^N}{N}$	0	$\frac{2^N}{N}$
$mnVA, m = 4, n = 2$	$2 * 2^k$	$2^k$	$2 * 2^k$	2	$2 * 2^k + \frac{2}{N}$
$mnVA, m = 5, n = 2$	$2 * 2^k + 4$	$2 * 2^k + 2$	$2 * 2^k + 4$	2	$2 * 2^k + 2 + \frac{2}{N}$
$mnVA, m = 6, n = 4$	$2 * 2^k + 8$	$2 * 2^k + 4$	$2 * 2^k + 8$	4	$2 * 2^k + 4 + \frac{4}{N}$

$k$  is the memory size of the codes,  $k = 2$  for eMiller codes, Miller codes and FM0/FM1 codes;  $N$  is the data block length.

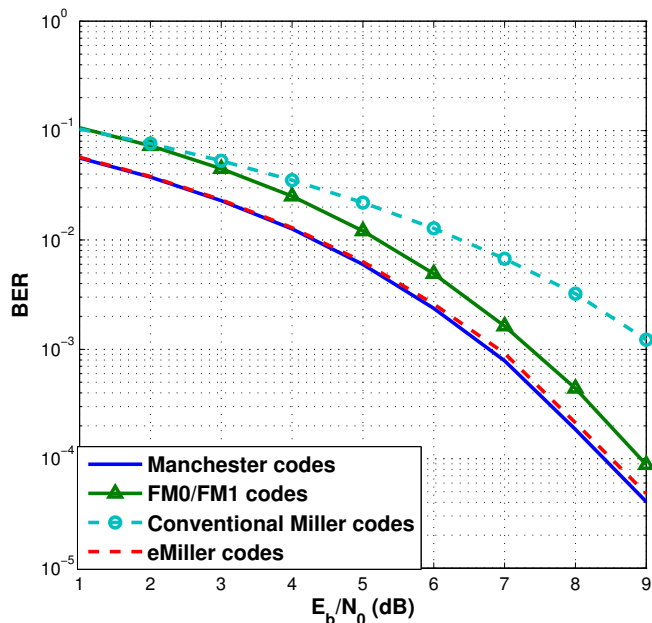


Fig. 11: BER of RLL codes over AWGN VLC channels. From top down: conventional Miller codes, FM0/FM1 codes, eMiller codes, and Manchester codes

is 60 degree, detector physical area of a PD is  $1 \text{ cm}^2$ . Data rate is 100 MB/s. Gain of an optical filter is 1, refractive index of a lens at a PD is 1.5.

We first evaluate the proposed eMiller codes and other RLL codes without the presence of channel coding. The data block length is set to 500 information bits. The conventional Miller code, FM0/FM1 codes and eMiller codes are decoded using the original Viterbi decoder ( $m = 4, n = 1$ ), while Manchester codes are decoded using the ML decoder. As shown in Fig. 11 and 12, the proposed eMiller codes significantly outperform conventional Miller codes and FM0/FM1 codes, and have the same performance as Manchester codes.

To verify the efficiency of the proposed  $mnVA$ , we present the performance of the channel-coded VLC system with the conventional Miller codes and the eMiller codes in Fig. 13 and 14, respectively. An RS(15,7) code over  $GF(2^4)$ , which is listed in the IEEE 802.15.7 VLC standard, is employed in the simulation; this is an FEC code, and the frame size is set to 700 information bits. We see that  $mnVA$  is not only effective

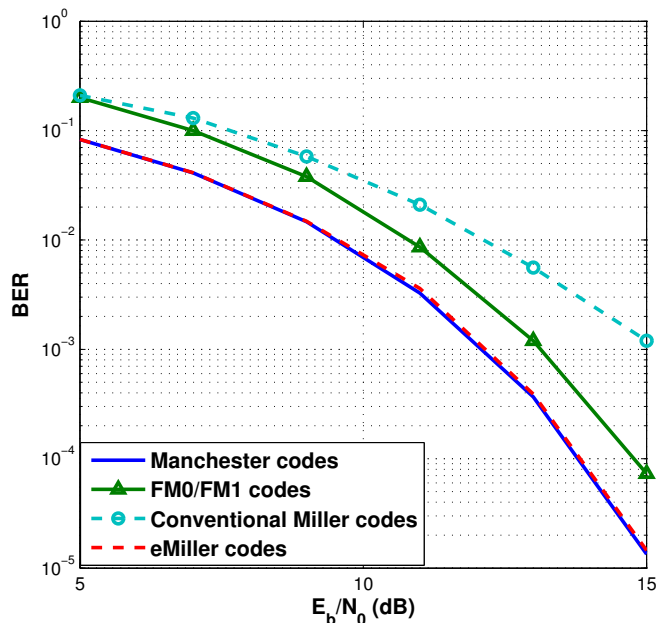


Fig. 12: BER of RLL codes over the practical VLC channels. From top down: conventional Miller codes, FM0/FM1 codes, eMiller codes, and Manchester codes

for eMiller codes but also for conventional Miller codes (in fact more so for the conventional case). It can be observed that barely increasing the number of the candidate (without saving additional survivors in the intermediate stages) at the final stage does not make much an improvement to the performance (see the dashed curves). However, preserving just one more survival path along the way (increasing  $m$  from 4 to 5) will quickly bring in noticeable performance gain of some 0.8 dB at BER of  $10^{-5}$  (see the solid curves). The performance can be further improved with more survival paths being preserved during the intermediate stages and the final stage (see dotted curves,  $m = 6$ ).

We also compare our RS-eMiller coding scheme with three other reported schemes: RS-Manchester scheme [1] with the BM and ML decoding, RS-4B6B scheme [21] with the BM and 16-candidate decoding (Note that the 4B6B codes have a code rate of  $2/3$  and a run-length limit of 4.), and RS-4B6B scheme [21] with the soft RS and SISO 4B6B decoding [22]. The block size is 700 information bits, and the overall rate

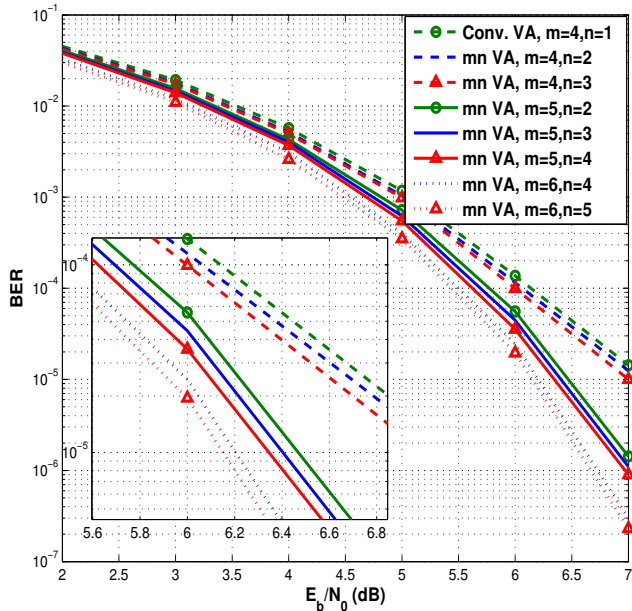


Fig. 13: BER of the proposed  $mn$ -Viterbi algorithm for decoding conventional Miller codes. Three sets of curves from top down: (i) dashed curves (worst set): no additional path was retained in any intermediate stages (i.e.,  $m = 4$ ) and decoder merely declares more survivors at the final stage; (ii) solid curves (middle set): one additional survival path was preserved in all the intermediate stages ( $m = 5$ ) and multiple outputs were produced in the final stage; (iii) dotted curves (best set): two additional survival paths were preserved in all the intermediate stages ( $m = 6$ ) and multiple outputs were produced in the final stage.

of these coded systems is either  $\frac{5}{15} \frac{4}{6} \approx 0.22$  (RS-4B6B) or  $\frac{7}{15} \frac{1}{2} \approx 0.23$  (others). As shown in Fig. 15, when conjunction with a hard RS decoder (BM decoding), RS-4B6B [21] scheme results in the worst performance; the next set is RS-eMiller scheme (using the conventional Viterbi algorithm) and RS-Manchester [1] scheme with the latter being slight better; and the best set is RS-eMiller scheme with  $mnVA$  decoding, which yields close to 1 dB gain over RS-4B6B and about 0.5 dB gain over RS-Manchester (at BER  $10^{-4}$ ). We also consider the soft RS decoding in our simulation results. The RS code is decoded using the same soft decoding as [22]. Since the eMiller code has an elegant trellis structure, we can use the BCJR algorithm to calculate the soft output (the *a posteriori* probability) of the codewords. The simulation results show that when conjunction with the soft RS decoder, our solution still clearly performs better than the RS-4B6B scheme in [22] because of the good error correction ability of the eMiller codes. The eMiller-4B6B with BCJR and soft RS decoding exhibits the best performance among all the schemes, but the soft RS decoder has a higher complexity than the BM decoder. Fig. 16 presents the BER performance of different cases under the actual VLC channel. Our proposed RS-eMiller scheme with  $mnVA$  decoding still shows the best performance among all the schemes with BM

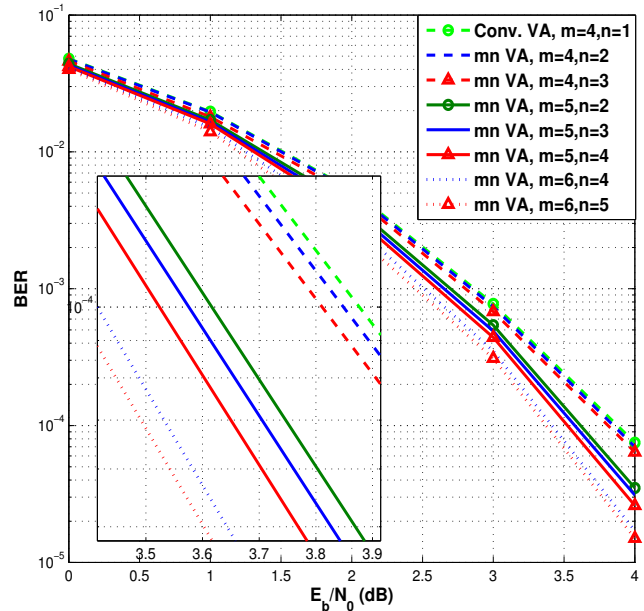


Fig. 14: BER of the proposed  $mn$ -Viterbi algorithm for decoding eMiller codes. Three sets of curves from top down: (i) dashed curves (worst set): no additional path was retained in any intermediate stages (i.e.,  $m = 4$ ) and decoder merely declares more survivors at the final stage; (ii) solid curves (middle set): one additional survival path was preserved in all the intermediate stages ( $m = 5$ ) and multiple outputs were produced in the final stage; (iii) dotted curves (best set): two additional survival paths were preserved in all the intermediate stages ( $m = 6$ ) and multiple outputs were produced in the final stage.

decoding. The gain over the conventional schemes is more compared to the AWGN cases, which is about 1.5 dB over RS-4B6B and about 0.9 dB gain over RS-Manchester (at BER  $10^{-4}$ ). Regarding the schemes with the soft RS decoding, our eMiller-RS codes is able to achieve about 1.3 dB gain (at BER  $10^{-4}$ ) over the RS-4B6B scheme in [22].

To further verify the effectiveness of the eMiller code, we test the performance of the eMiller codes when being used in the VLC architecture in [23]. A concatenated RLL-convolutional coded structure with an iterative decoding scheme is investigated in [23]. The data block length is set to 150. (5, 7) convolutional codes (CC) is used as the FEC. Fig. 17 demonstrates the eMiller-CC codes without iterative decoding clearly outperform the Miller-CC codes with one iteration in [23]. By iteratively decoding the eMiller code and the convolutional code once, we can get better performance than the Miller-CC codes with 4-iteration decoding.

## VII. CONCLUSION

Run-length limited coding is indispensable to avoid LED flicker and ensure DC (direct current) balance in visible light communications, but is much under-studied. This paper investigates Miller codes, a class of RLL codes known for

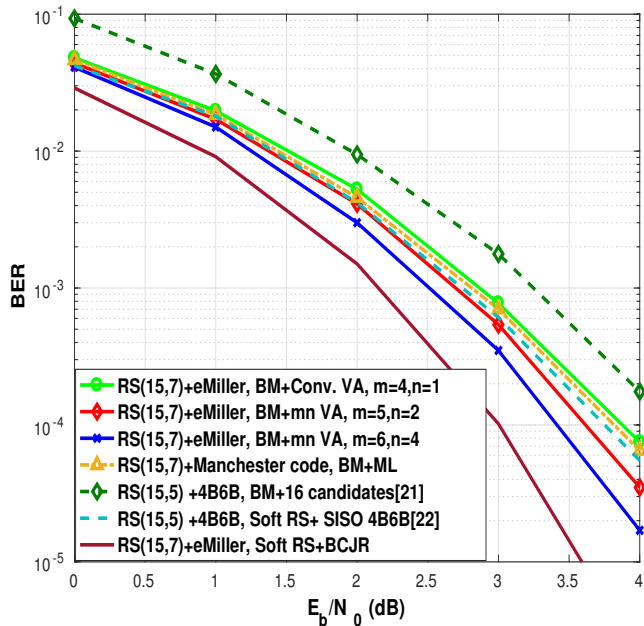


Fig. 15: BER comparison of eMiller codes with existing schemes in the presence of RS channel coding under the AWGN VLC channel. From worst to best: RS-4B6B (BM+16 candidates), RS-eMiller (BM+conventional VA), RS-Manchester (BM+ML), RS-4B6B (Soft RS+ SISO 4B6B), RS-eMiller ( $mnVA$ , with  $m=5, n=2$ ), RS-eMiller ( $mnVA$ , with  $m=6, n=4$ ) and RS-eMiller (Soft RS + BCJR)

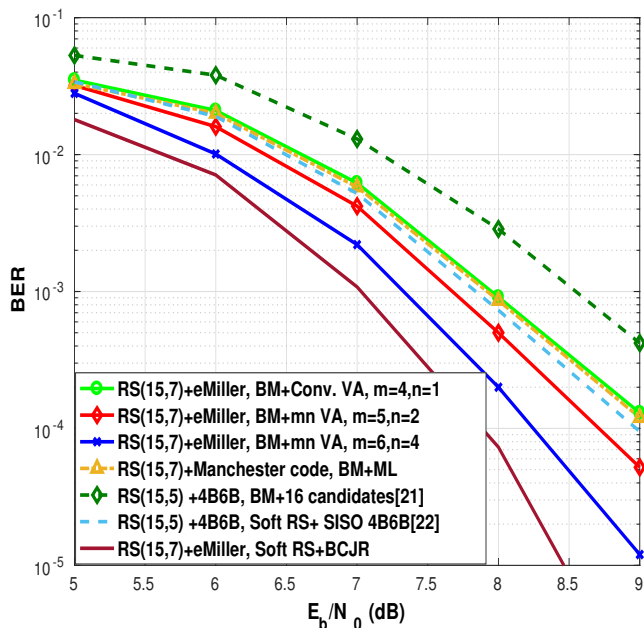


Fig. 16: BER comparison of eMiller codes with existing schemes in the presence of RS channel coding under the practical VLC channel. From worst to best: RS-4B6B (BM+16 candidates), RS-eMiller (BM+conventional VA), RS-Manchester (BM+ML), RS-4B6B (Soft RS+ SISO 4B6B), RS-eMiller ( $mnVA$ , with  $m=5, n=2$ ), RS-eMiller ( $mnVA$ , with  $m=6, n=4$ ) and RS-eMiller (Soft RS + BCJR)

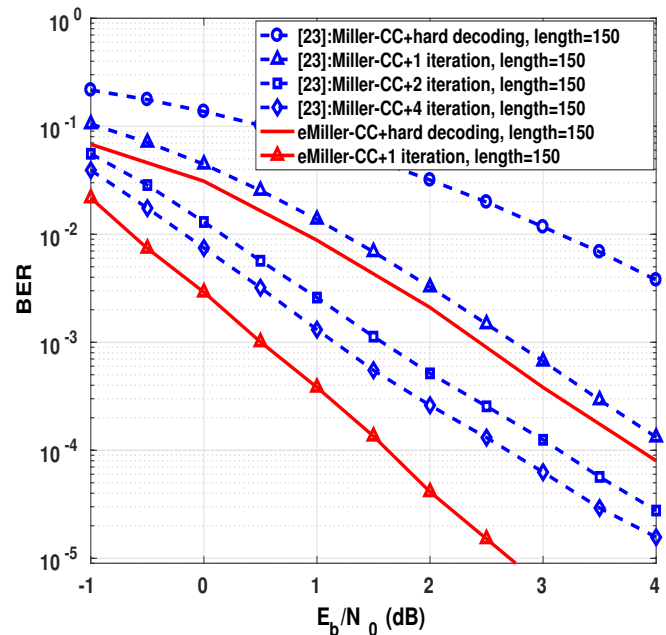


Fig. 17: BER comparison of eMiller codes with existing schemes [23] in the presence of (5,7) convolutional coding under the AWGN VLC channel.

high bandwidth efficiency (but less desirable power efficiency), for use in VLC. The key contribution is the invention of a new type of enhanced Miller codes that offer considerably better power efficiency than the conventional ones. Dimming and flicker control is analyzed, power spectral density and minimum Hamming distance are calculated, and the performance of eMiller codes is evaluated both by themselves and in use with Reed-Solomon codes. In addition to the conventional Viterbi algorithm (VA), we also present a simple but useful modification that preserves multiple survival paths at each decoding stage. The modified VA, termed  $mnVA$ , helps further improve the performance of eMiller codes with little additional computational complexity. Comparison with a variety of existing RLL codes including Manchester codes, FM0/FM1 codes, and 4B6B codes clearly establishes eMiller codes as a highly promising candidate for VLC application in future.

## REFERENCES

- [1] A. Sendonaris, E. Erkip, and B. Aazhang, "IEEE 802.15.7 Visible light communication: modulation schemes and dimming support," *IEEE Commun. Magazine*, vol. 50, no. 3, pp. 72-82, March. 2012.
- [2] T. Komine and M. Nakagawa, "Fundamental analysis for visible light communication system using LED lights," *IEEE Trans. on Consumer Electronics*, vol. 50, no. 1, pp. 100-107, Feb. 2004.
- [3] J. Gancarz, H. Elgala, and T. D. C. Little, "Impact of lighting requirements on VLC systems," *IEEE Commun. Magazine*, vol. 51, no. 12, pp. 34-41, Dec. 2013.
- [4] H. Elgala, R. Mesleh, and H. Haas, "Indoor optical wireless communication: potential and state-of-the-art," *IEEE Commun. Magazine*, vol. 49, no. 9, pp. 56-62, Dec. 2011.
- [5] S. Zhang, S. Watson, J.J.D. McKendry, D. Massoubre, A. Cogman, E. Gu, R.K. Henderson, A.E. Kelly, and M.D. Dawson, "1.5 Gbit/s Multi-Channel Visible Light Communications Using CMOS Controlled GaN-Based LEDs," *J. Lightwave Technol.*, vol. 31, no.8, pp.1211-1216, 2013.

- [6] A. Jovicic, J. Li, and T. Richardson, "Visible light communication: opportunities, challenges and the path to market," *IEEE Commun. Magazine*, vol. 51, no. 12, pp. 26-32, Dec. 2013.
- [7] M. Noshad and M. B. Pearce, "Application of expurgated PPM to indoor visible light communications-Part I: single-user systems," *Journal of Lightwave Tech.*, vol. 32, no. 5, pp. 875-882, March. 2014.
- [8] M. Noshad and M. B. Pearce, "Application of expurgated PPM to indoor visible light communications-Part II: access networks," *Journal of Lightwave Tech.*, vol. 32, no. 5, pp. 883-890, March. 2014.
- [9] D. Xiong, *Digital Modulation Techniques*, Norwood, MA: Artech House, 2000.
- [10] A. B. Siddique and M. Tahir, "Joint rate-brightness control using variable rate MPPM for LED based visible light communication systems," *IEEE Trans. on Wireless Comm.*, vol. 12, no. 9, pp. 4604-4611, Sep. 2013.
- [11] *IEEE Standard for Local and Metropolitan Area Networks-Part 15.7: Short-Range Wireless Optical Communication Using Visible Light*, IEEE Standard 802.15.7, 2011, pp.248-271.
- [12] S. Kim, and S. Jung "Novel FEC coding scheme for dimmable visible light communication based on the modified Reed-Muller codes," *IEEE Photonics Tech. Letters*, vol. 23, no. 20, pp. 1514-1516, Oct. 2011.
- [13] S. Kim and S. Jung, "Modified Reed-Muller coding scheme made from the bent function for dimmable visible light communications," *IEEE Photonics Tech. Letters*, vol. 25, no. 1, pp. 11-13, Jan. 2013.
- [14] J. Kim and H. Park, "A coding scheme for visible light communication with wide dimming range," *IEEE Photonics Tech. Letters*, vol. 26, no. 5, pp. 465-468, March 2014.
- [15] S. Kim, "Adaptive FEC codes suitable for variable dimming values in visible light communication," *IEEE Photonics Tech. Letters*, vol. 27, no. 9, pp. 967-969, May. 2015.
- [16] S. Lee and J.K. Kwon, "Turbo code-based error correction scheme for dimmable visible light communication systems," *IEEE Photonics Tech. Letters*, vol. 24, no. 17, pp. 1463-1465, Sep. 2012.
- [17] P. Perry, M. Li, M. Lin and Z. Zhang, "Runlength limited codes for single error-detection and single error-correction with mixed type errors," *IEEE Trans. on Info. Theory*, vol. 44, no. 4, pp. 1588-1592, July 1998.
- [18] A. J. van Wijngaarden and K. A. S. Immink, "Construction of maximum run-length limited codes using sequence replacement techniques," *IEEE Journal of Selected Areas in Comm.*, vol. 28, no. 2, pp. 200-207, Feb. 2010.
- [19] H. Chen, H. Chou, M. Lin and S. Lee, "Capacity approaching run-length-limited codes for multilevel recording systems," *IEEE Trans. on Magnetics*, vol. 46, no. 1, pp. 95-104, Jan. 2010.
- [20] A. Bletsas, J. Kimionis, A. G. Dimitriou, and G.N. Karystinos, "Single-antenna coherent detection of collided FM0 RFID signals," *IEEE Trans. on Comm.*, vol. 60, no. 3, pp. 756-766, 2012.
- [21] H. Wang and S. Kim, "New RLL decoding algorithm for multiple candidates in visible light communication," *IEEE Photonics Tech. Letters*, vol. 27, no. 1, pp. 15-17, Jan. 2015.
- [22] H. Wang and S. Kim, "Soft-Input Soft-Output Run-Length Limited Decoding for Visible Light Communication," *IEEE Photonics Technology Letters*, vol. 28, no. 3, pp. 225-228, Feb. 2016
- [23] X. Lu and J. Li, "Achieving FEC and RLL for VLC: A concatenated convolutional-Miller coding mechanism," *IEEE Photonics Tech. Letters*, vol. 28, no. 9, pp. 1030-1033, May, 2016.
- [24] M. Hecht and A. Guida, "Delay modulation," *Proceedings of the IEEE*, vol. 57, no. 7, pp. 1314-1316, 1969.
- [25] A. Cailean, B. Cagneau, L. Chassagne, V. Popa, and M. Dimian "Evaluation of the noise effects on Visible Light Communications using Manchester and Miller coding," *12th International Conf. on Dev. and App. systems*, Romania, pp. 85-89, 2014.
- [26] M. Simon and D. Divsalar, "Some interesting observations for certain line codes with application to RFID," *IEEE Trans. on Comm.*, vol. 54, no. 4, pp. 583-586, April. 2006.
- [27] C. Xiong and Z. Yan, "Improved Iterative Hard- and Soft-Reliability Based Majority-Logic Decoding Algorithms for Non-Binary Low-Density Parity-Check Codes," *IEEE Trans. on Signal Processing*, vol. 62, no. 20, pp. 5449-5457, Oct. 2014.